INTERNATIONAL JOURNAL FOR NUMERICAL METHODS IN FLUIDS
Int. J. Numer. Meth. Fluids 2008; **56**:629–641
Published online 19 June 2007 in Wiley InterScience (www.interscience.wiley.com). DOI: 10.1002/fld.1543

Introducing unsteady non-uniform source terms into the lattice Boltzmann model

Yongguang Cheng*,† and Jinping Li

State Key Laboratory of Water Resources and Hydropower Science, Wuhan University, Wuhan 430072, China

SUMMARY

Taking body forces into account is not new for the lattice Boltzmann method, yet most of the existing approaches can only treat steady and uniform body forces. To manage situations with time- and space-dependent body forces or source terms, this paper proposes a new approach through theoretical derivation and numerical verification. The method by attaching an extra term to the lattice Boltzmann equation is still used, but the expression of the extra term is modified. It is the modified extra term that achieves the particularity of the new approach. This approach can not only introduce unsteady and non-uniform body forces into momentum equations, but is also able to add an arbitrary source term to the continuity equation. Both the macroscopic equations from multi-scale analysis and the simulated results of typical examples show that the accuracy with second-order convergence can be guaranteed within incompressible limit. Copyright © 2007 John Wiley & Sons, Ltd.

Received 5 March 2007; Revised 8 May 2007; Accepted 12 May 2007

KEY WORDS: lattice Boltzmann method; source term; unsteady; non-uniform; BGK model

1. INTRODUCTION

As a new scheme for simulating fluid flows, the lattice Boltzmann method (LBM) has been effectively applied to model many fluid flow phenomena, Newtonian or non-Newtonian, multi-component or multi-phase, compressible or incompressible, and has been applied successfully to technical simulations, such as aerodynamic, aeroacoustic, thermodynamic, chemical reactive and

*Correspondence to: Yongguang Cheng, State Key Laboratory of Water Resources and Hydropower Science, Wuhan University, Wuhan 430072, China.
†E-mail: chengyg2004@yahoo.com.cn

Contract/grant sponsor: National Natural Science Foundation of China; contract/grant numbers: 50009007, 10572106
Contract/grant sponsor: Scientific Research Foundation for Returned Overseas Chinese Scholars, State Education Ministry, China

hydraulic problems [1–10]. The rapid increase in the number of published works on LBM in recent years boosts the perspective of practical applications.

In some simulations, for example, the simulation of water waves, gravitational or body force is important and should be considered. To yield correct macroscopic momentum equations with specific body forces, some modifications to LBM have been proposed [11–13]. In [11], a simple extra term was attached to the right side of the lattice Boltzmann equation (LBE), and from the modified LBE the Navier–Stokes (NS) equations with the exact force term were derived. The feasibility and accuracy of this particular approach were verified by analytical solutions of the force-driven Poiseuille flow and the Couette flow. In [12], a more detailed derivation of the LBM model with a force term was conducted from the Enskog equation, and a second-order expression of the discretized lattice force function was presented. More specially, Buick and Greated [13] reviewed the gravity in LBM, and analysed four methods to modify the fluid momentum, which includes combining the gravity term with the pressure tensor, calculating the equilibrium distribution with an altered velocity, adding an additional term to LBE, as well as the composition of the former three. Following the methods in [12, 13], Li and Kwok [14] proposed a high Reynolds number LBM with external forces for microfluidics, Guo *et al.* [15] analysed the effects of discrete lattice on the force term in LBM, Chen *et al.* [16] compared the accuracy of two types of force term functions, and Lu and Zhan [17] introduced analogous approaches into the finite difference LBM.

All the above works are profound and valuable, however, there are a few of them capable of treating unsteady and non-uniform forces with a convergence higher than a first order, because in the above-mentioned works the acceleration is viewed as constant in analysis. But in practical simulations, the space- and time-dependent forces in the fluid momentum often encounter, for instance, frictional loss of head in the water hammer simulation [9] and resistance in the shallow water wave simulation [10], which are all unsteady or non-uniform. On the other hand, when there are discharge inflows or outflows in the middle of an open channel flow [18], a source term in the continuity equation may appear. Another typical example of an unsteady and non-uniform force exists in the immersed boundary method [19], a fluid–structure interaction (FSI) model for biological problems. In the immersed boundary method, LBM has been utilized to model the fluid simulation part [20] due to its superior efficiency. To be suitable for fluid–structure coupling, the ability to accurately deal with the unsteady and non-uniform force imposed on the fluid by the structure must be provided. Unfortunately, the only work on the variable body force or source term in LBM to date might be [21], in which a specific set of equations with source terms was solved by adding a case-dependent extra term to LBE. Because the method in [21] is not suitable for the above-mentioned problems, it is necessary to find a new approach.

In this paper, a general approach to consider the unsteady and non-uniform source terms in the momentum and continuity equations of fluid flow by LBM is proposed. The theoretical derivation will be presented in the next section, and the typical example verification will be conducted in the third section.

2. THEORETICAL DERIVATION

To present the proposed approach logically, errors of a typical existing approach will be analysed at first, and then the new idea will be elucidated based on the derivation and prepared associated formulae.

DOI: 10.1002/fld

2.1. Errors using the existing approach

One of the most common approaches to consider the effect of body forces is by attaching an additional term to the standard LBE, such as in [11]

$$f_\alpha(\mathbf{x}+\mathbf{e}_\alpha\delta_t, t+\delta_t) - f_\alpha(\mathbf{x}, t) = -\frac{1}{\tau}[f_\alpha(\mathbf{x}, t) - f_\alpha^{(0)}(\mathbf{x}, t)] + \delta_t g_\alpha(\mathbf{x}, t) \tag{1}$$

where f_α is the particle velocity distribution function along the αth particle velocity direction, $f_\alpha^{(0)}$ the equilibrium distribution function, g_α the forcing term function, τ the relaxation factor, $\mathbf{e}_\alpha$ the discrete particle vector, x the lattice grid and δ_t the time increment. All the distribution and equilibrium distribution functions are the same as those without body force, and the only difference to the standard LBE is that lattice force function g_α is added in (1).

Equation (1) is very convenient to be used and quite accurate for steady source term situations [3]. However, it may lead to errors when unsteady or non-uniform source terms are considered. To prove this, the corresponding macroscopic equations of (1) will be derived based on the Chapman–Enskog expansion procedure as in [1, 22].

The distribution function and time differential may be expressed as the expansions with Knudson number $\varepsilon \ll 1$, as follows:

$$f_\alpha = f_\alpha^{(0)} + \varepsilon f_\alpha^{(1)} + \varepsilon^2 f_\alpha^{(2)} + O(\varepsilon^3), \quad \frac{\partial}{\partial t} = \frac{\partial}{\partial t_0} + \varepsilon\frac{\partial}{\partial t_1} + \varepsilon^2\frac{\partial}{\partial t_2} + O(\varepsilon^3) \tag{2}$$

If the density and momentum are defined as

$$\rho = \sum_\alpha f_\alpha = \sum_\alpha f_\alpha^{(0)}, \quad \rho u_i = \sum_\alpha e_{\alpha i} f_\alpha = \sum_\alpha e_{\alpha i} f_\alpha^{(0)} \tag{3}$$

one can find

$$\sum_\alpha f_\alpha^{(n)} = 0, \quad \sum_\alpha e_{\alpha i} f_\alpha^{(n)} = 0 \quad (n = 1, 2, \ldots) \tag{4}$$

where i is the indication of ith direction of the coordinates.

Through the Taylor expansion of the left side of (1), one may obtain:

$$\delta_t\left(\frac{\partial}{\partial t} + e_{\alpha j}\frac{\partial}{\partial x_j}\right) f_\alpha + \frac{1}{2}\delta_t^2\left(\frac{\partial}{\partial t} + e_{\alpha j}\frac{\partial}{\partial x_j}\right)^2 f_\alpha + O(\delta_t^3) = -\frac{1}{\tau}(f_\alpha - f_\alpha^{(0)}) + \delta_t g_\alpha \tag{5}$$

Inserting (2) into (5) and assuming $\delta_t = \varepsilon$, one may get the ε-order scale equation

$$\left(\frac{\partial}{\partial t_0} + e_{\alpha j}\frac{\partial}{\partial x_j}\right) f_\alpha^{(0)} = -\frac{1}{\tau} f_\alpha^{(1)} + g_\alpha \tag{6}$$

and ε^2-order scale equation:

$$\frac{\partial}{\partial t_1} f_\alpha^{(0)} + \left(1 - \frac{1}{2\tau}\right)\left(\frac{\partial}{\partial t_0} + e_{\alpha j}\frac{\partial}{\partial x_j}\right) f_\alpha^{(1)} + \frac{1}{2}\left(\frac{\partial}{\partial t_0} + e_{\alpha j}\frac{\partial}{\partial x_j}\right) g_\alpha = -\frac{1}{\tau} f_\alpha^{(2)} \tag{7}$$

Considering (4), the summation of (6) and summation of (6) $\cdot\, e_{\alpha i}$ over α can result in

$$\frac{\partial \rho}{\partial t_0} + \frac{\partial(\rho u_j)}{\partial x_j} = A \tag{8}$$

DOI: 10.1002/fld

$$\frac{\partial(\rho u_i)}{\partial t_0} + \frac{\partial \Pi_{ij}^{(0)}}{\partial x_j} = B_i \tag{9}$$

in which

$$A = \sum_\alpha g_\alpha, \quad B_i = \sum_\alpha e_{\alpha i} g_\alpha, \quad \Pi_{ij}^{(0)} = \sum_\alpha e_{\alpha i} e_{\alpha j} f_\alpha^{(0)} \tag{10}$$

Similarly, the summations of (7) and (7) $\cdot\, e_{\alpha i}$ over α yield

$$\frac{\partial \rho}{\partial t_1} + \frac{1}{2}\left(\frac{\partial A}{\partial t_0} + \frac{\partial B_j}{\partial x_j}\right) = 0 \tag{11}$$

$$\frac{\partial(\rho u_i)}{\partial t_1} + \left(1 - \frac{1}{2\tau}\right)\frac{\partial}{\partial x_j}\Pi_{ij}^{(1)} + \frac{1}{2}\left(\frac{\partial B_i}{\partial t_0} + \frac{\partial C_{ij}}{\partial x_j}\right) = 0 \tag{12}$$

where

$$C_{ij} = \sum_\alpha e_{\alpha i} e_{\alpha j} g_\alpha, \quad \Pi_{ij}^{(1)} = \sum_\alpha e_{\alpha i} e_{\alpha j} f_\alpha^{(1)} \tag{13}$$

Following the same derivation procedure of the standard LBM model, one can get

$$\Pi_{ij}^{(0)} = C_s^2 \rho \delta_{ij} + \rho u_i u_j \tag{14}$$

and

$$\Pi_{ij}^{(1)} = -\tau\{\tfrac{2}{3}\rho S_{ij} + (C_s^2 A)\delta_{ij} + (u_i B_j + u_j B_i - C_{ij})\} + O(M^3) \tag{15}$$

in which $S_{ij} = \frac{1}{2}(\partial u_i/\partial x_j + \partial u_j/\partial x_i)$.

Therefore, combination of (8) $+ \varepsilon \times$ (11) and (9) $+ \varepsilon \times$ (12) with $\varepsilon = \delta_t$ can result in

$$\frac{\partial \rho}{\partial t} + \frac{\partial(\rho u_j)}{\partial x_j} = A - \frac{1}{2}\left(\frac{\partial A}{\partial t_0} + \frac{\partial B_j}{\partial x_j}\right)\delta_t + O(\delta_t^2) \tag{16}$$

$$\frac{\partial(\rho u_i)}{\partial t} + \frac{\partial(\rho u_i u_j)}{\partial x_j} = B_i - \frac{\partial p}{\partial x_i} + 2\nu\frac{\partial}{\partial x_j}(\rho S_{ij}) + 3\nu\frac{\partial(C_s^2 A)}{\partial x_i} - 3\nu\frac{\partial C_{ij}}{\partial x_j}$$
$$+3\nu\frac{\partial}{\partial x_j}(u_j B_i + u_i B_j) - \frac{1}{2}\left(\frac{\partial B_i}{\partial t_0} + \frac{\partial C_{ij}}{\partial x_j}\right)\delta_t + O(\delta_t^2) + O(M^3) \tag{17}$$

where $p = C_s^2 \rho$, $\nu = ((2\tau - 1)/6)\delta_t$, $C_s^2 = \frac{1}{3}$ and M the Mach number.

Equations (16) and (17) are the corresponding macroscopic equations of (1). For steady and uniform source term situations, the derivatives of A, B_i and C_{ij} are zero, and therefore the extra terms, i.e. the second term on the right side of (16) and the fourth to seventh terms on the right side of (17), should be zero. That is to say, the LBE (1) can approximate NS equations with a second-order accuracy in incompressible limit as long as the source terms are steady and uniform. This is why the existing approach is accurate for steady and uniform body forces. But for situations when source terms are unsteady or non-uniform, the extra terms in Equations (16) and (17) will result in errors, even though the errors may be neglectable sometimes.

DOI: 10.1002/fld

2.2. The new approach

To eliminate the error terms in (16) and (17), a modification to LBE (1) should be made. In the new approach, the LBE with source term effect is rewritten as:

$$f_\alpha(\mathbf{x}+\mathbf{e}_\alpha\delta_t, t+\delta_t) - f_\alpha(\mathbf{x}, t) = -\frac{1}{\tau}[f_\alpha(\mathbf{x}, t) - f_\alpha^{(0)}(\mathbf{x}, t)] + \frac{\delta_t}{2}[g_\alpha(\mathbf{x}, t) + g_\alpha(\mathbf{x}+\mathbf{e}_\alpha\delta_t, t+\delta_t)] \tag{18}$$

Accordingly, Equation (5) becomes:

$$\delta_t\left(\frac{\partial}{\partial t}+e_{\alpha j}\frac{\partial}{\partial x_j}\right)f_\alpha + \frac{1}{2}\delta_t^2\left(\frac{\partial}{\partial t}+e_{\alpha j}\frac{\partial}{\partial x_j}\right)^2 f_\alpha + O(\delta_t^3) = -\frac{1}{\tau}(f_\alpha - f_\alpha^{(0)}) + \delta_t g_\alpha + \frac{\delta_t^2}{2}\left(\frac{\partial}{\partial t}+e_{\alpha j}\frac{\partial}{\partial x_j}\right)g_\alpha \tag{19}$$

Therefore, the g_α terms in (7) can be counteracted, and (7) changes to:

$$\frac{\partial}{\partial t_1}f_\alpha^{(0)} + \left(1-\frac{1}{2\tau}\right)\left(\frac{\partial}{\partial t_0}+e_{\alpha j}\frac{\partial}{\partial x_j}\right)f_\alpha^{(1)} = -\frac{1}{\tau}f_\alpha^{(2)} \tag{20}$$

As a result, (11) and (12) become:

$$\frac{\partial \rho}{\partial t_1} = 0 \tag{21}$$

$$\frac{\partial(\rho u_i)}{\partial t_1} + \left(1-\frac{1}{2\tau}\right)\frac{\partial}{\partial x_j}\Pi_{ij}^{(1)} = 0 \tag{22}$$

If we specially redefine

$$A = \sum_\alpha g_\alpha, \quad B_i = \sum_\alpha e_{\alpha i} g_\alpha, \quad C_{ij} = \sum_\alpha e_{\alpha i} e_{\alpha j} g_\alpha = u_i B_j + u_j B_i + C_s^2 A\delta_{ij} \tag{23}$$

then, Equations (16) and (17) change to:

$$\frac{\partial \rho}{\partial t} + \frac{\partial(\rho u_j)}{\partial x_j} = A + O(\delta_t^2) \tag{24}$$

$$\frac{\partial(\rho u_i)}{\partial t} + \frac{\partial(\rho u_i u_j)}{\partial x_j} = B_i - \frac{\partial p}{\partial x_i} + 2\nu\frac{\partial}{\partial x_j}(\rho S_{ij}) + O(\delta_t^2) + O(M^3) \tag{25}$$

Obviously, (24) and (25) approximate the incompressible NS equations with a second order of convergence.

DOI: 10.1002/fld

At this stage, the new approach may be defined as: utilizing LBE (18), satisfying constraints (23) and achieving the corresponding macroscopic equations (24) and (25).

The expression of g_α for a specific lattice Boltzmann model can be determined based on the constraints in (23). For example, considering the typical two-dimensional model D2Q9 and typical three-dimensional model D3Q15 in Reference [1], g_α may take the form

$$g_\alpha = w_\alpha\{A + 3\mathbf{B}\cdot[(\mathbf{e}_\alpha - \mathbf{u}) + 3(\mathbf{e}_\alpha\cdot\mathbf{u})\mathbf{e}_\alpha]\} \tag{26}$$

in which

$$w_\alpha = \begin{cases} \frac{4}{9}, & \alpha = 0 \\ \frac{1}{9}, & \alpha = 1,2,3,4 \\ \frac{1}{36}, & \alpha = 5,6,7,8 \end{cases} \text{ for D2Q9 and } w_\alpha = \begin{cases} \frac{2}{9}, & \alpha = 0 \\ \frac{1}{9}, & \alpha = 1,2,\ldots,6 \\ \frac{1}{72}, & \alpha = 7,8,\ldots,14 \end{cases} \text{ for D3Q15}$$

Because Equation (18) is implicit owing to $g_\alpha(\mathbf{x} + \mathbf{e}_\alpha\delta_t, t + \delta_t)$, an iteration procedure should be used at each time march step.

3. NUMERICAL VERIFICATION

3.1. Description of a verification example

To verify the above theoretical derivation, the selected benchmark examples should have analytical solutions or highly accurate numerical solutions. Therefore, the steady and unsteady flows in a three-dimensional duct are specially designed and simulated in this section. As shown in Figure 1, the duct has a constant width, with height varying in the third direction. This example is typical because when the flow is projected to the x_1x_2 plane, the governing equations of the flow in two-dimensional form will have unsteady and non-uniform source terms for both continuity and

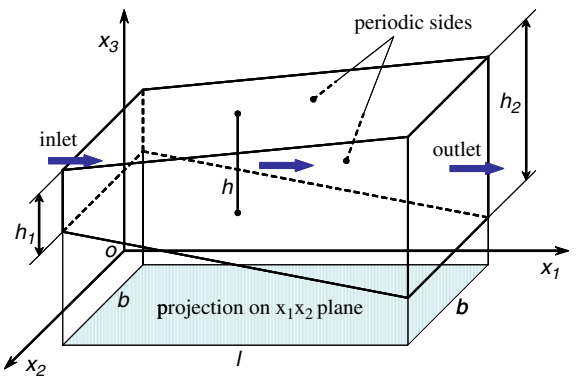

Figure 1. Schematic of the duct flow.

DOI: 10.1002/fld

momentum equations, which may be expressed as [23]

$$\frac{\partial \rho}{\partial t} + \frac{\partial(\rho u_j)}{\partial x_j} = -\frac{a_j}{h}(\rho u_j) \tag{27}$$

$$\frac{\partial(\rho u_i)}{\partial t} + \frac{\partial(\rho u_i u_j)}{\partial x_j} = -\frac{\partial p}{\partial x_i} + 2\nu \frac{\partial}{\partial x_j}\left[\rho\left(S_{ij} - \frac{1}{3}S_{kk}\delta_{ij}\right)\right] - \frac{a_j}{h}(\rho u_i u_j) \tag{28}$$

in which $a_j = \partial h/\partial x_j$, $j = 1, 2$ and h is the height of the duct. It can be seen that $-(a_j/h)(\rho u_j)$ is the source of the continuity equation and $-(a_j/h)(\rho u_i u_j)$ is the source of the momentum equation. These two terms depend on both space and time. Apart from these, Equations (27) and (28) are the exact standard NS equation set.

It is noticeable that Equation (28) has S_{kk} in the viscosity term, but the corresponding momentum equation (25) in the above section does not. In order to conduct the comparison between the LBM simulations and the analytical solutions of the duct flow problem conveniently, S_{kk} in (28) is omitted in the following analysis.

Considering the two periodic sides, the flow can be uniform in the x_2-direction, therefore, the flow becomes one-dimensional. If incompressibility is further assumed, the governing equations with S_{kk} omitted change to [23]:

$$\frac{\partial p}{\partial t} + C_2^2 \frac{\partial(\rho_0 u)}{\partial x} = -\frac{C_2^2 \rho_0 u}{h}\frac{\partial h}{\partial x} \tag{29}$$

$$\frac{\partial(\rho_0 u)}{\partial t} + \frac{\partial(\rho_0 u^2)}{\partial x} = -\frac{\partial p}{\partial x} + 2\nu\rho_0 \frac{\partial^2 u}{\partial x^2} - \frac{\rho_0 u^2}{h}\frac{\partial h}{\partial x} \tag{30}$$

Though one-dimensional, this example may be the most suitable example we find for verification. It has unsteady and non-uniform source terms, especially, one can obtain analytical solutions for it, which are necessary for convergence analysis of a numerical scheme.

3.2. Steady flow

In a steady condition, (29) and (30) may reduce to:

$$\frac{\partial u}{\partial x} = \frac{u}{h}\frac{\partial h}{\partial x} \tag{31}$$

$$\rho_0 \frac{\partial}{\partial x}\left(\frac{u^2}{2}\right) = -\frac{\partial p}{\partial x} + 2\nu\rho_0 \frac{\partial^2 u}{\partial x^2} \tag{32}$$

Subsequently, with inlet height h_1, outlet height h_2 and slope $\partial h/\partial x = a = \text{const}$ are specified, one may obtain the analytical solutions

$$u(x) = \frac{h_2 u_2}{h_1 + ax} \tag{33}$$

$$p(x) = p_1 + \frac{\rho_0 h_2 u_2}{2}(h_2 u_2 + 4\nu a)\left[\frac{1}{h_1^2} - \frac{1}{(h_1 + ax)^2}\right] \tag{34}$$

in which u is the velocity and p is the pressure.

DOI: 10.1002/fld

Table I. Comparison of LBM and analytical results of steady duct flow.

Cases	Parameters							Methods	Results	
	ρ_0	v	h_1	h_2	a	p_1	u_2		p_2	u_1
A	1.0	3.0	1.0	1.2	0.01	1.0	0.1	Analytical	1.00440000	0.12000000
								Simulated	1.00423727	0.12000036
B	1.0	3.0	1.0	1.2	0.01	1.0	−0.1	Analytical	1.00000000	−0.12000000
								Simulated	1.00016275	−0.12000036
C	1.0	2.0	1.0	1.4	0.02	1.0	0.1	Analytical	1.01028571	0.14000000
								Simulated	1.00978433	0.14000245
D	1.0	1.0	1.0	0.4	−0.03	1.0	0.1	Analytical	1.00840000	0.04000000
								Simulated	1.00763000	0.03999435
E	1.0	0.3	1.0	0.4	−0.03	1.0	0.1	Analytical	0.99958000	0.04000000
								Simulated	0.99934646	0.03999443
F	1.0	2.0	1.0	1.4	0.02	1.0	0.01	Analytical	1.00059657	0.01400000
								Simulated	1.00059442	0.01400025

Model D2Q9 is used to simulate the problem through the two-dimensional approach. Source terms $A = -(a_j/h)(\rho u_j)$ and $B_i = -(a_j/h)(\rho u_i u_j)$ are chosen. The simulation domain is discretized by a lattice resolution of 20 in the x-direction and 10 in the y-direction. For boundary conditions, pressure, velocity and periodic condition are specified at the inlet, outlet and both lateral sides, respectively.

Table I presents the results of model D2Q9, compared with the analytical solution of formulae (33) and (34). Six cases of different parameters are chosen to analyse the effects of different a, v and u_2.

3.2.1. Analysis of influence on accuracy. Case A is selected to test the expansion flow with a moderate $a = 0.01$, while Case B is selected to test the contraction flow. The two cases are the same in geometry, and the only difference is in the flow direction of inlet velocity u_2. Comparing the simulated results with the analytical results, one knows that p_2 errors are in the 10^{-3} degree and u_1 errors in the 10^{-6} degree for both cases. To test the effect of expansion, Case C with a larger $a = 0.02$ is designed. The velocity and pressure distributions of this highly expanded case are shown in Figure 2, in which an increasing p and a declining u along x can be seen, and a good agreement of u and the cognizable deviation of p is evident. Case D is used to test the high contraction flow with $a = -0.03$ and its results are shown in Figure 3, in which both p and u increase along x, and the deviation of p is also apparent. It is clear that Case C and Case D have similar error degrees, namely 10^{-2} for p_2 and 10^{-5} for u_1. To improve the results of Case D, a smaller viscosity $v = 0.3$ is chosen and a slight better agreement of p_2 is obtained. The above analysis, along with Figures 2 and 3, suggests that the velocity error is small but the pressure error is relatively large, and that a, v and u_2 do not have a significant effect on error degrees.

DOI: 10.1002/fld

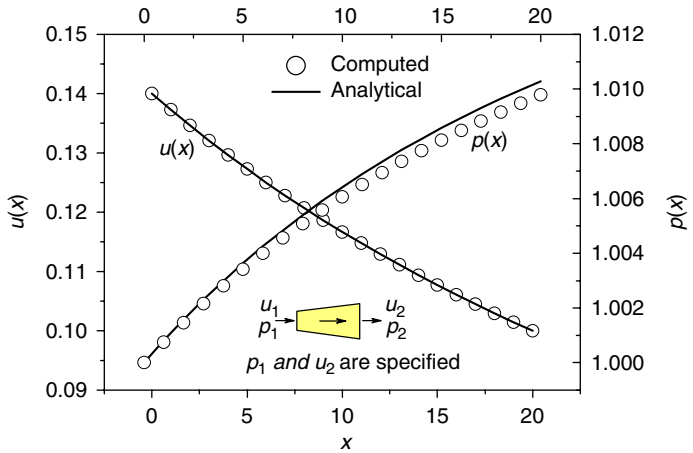

Figure 2. Velocity and pressure distributions in Case C.

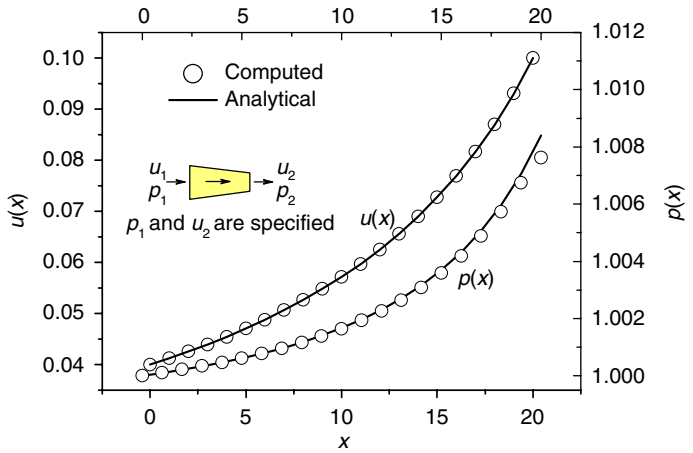

Figure 3. Velocity and pressure distributions in Case D.

Recalling the momentum equations (25) and (30), one may find that the compressibility of the LBM model is the main reason for pressure deviations. Therefore, in Case F the inlet velocity is reduced to $u_2 = 0.01$, and thereby a smaller error degree 10^{-5} of p_2 is achieved. To compare with Figure 2, the results of Case F are drawn in Figure 4, where a much better agreement of p is evident.

To quantitatively analyse the errors, we define the relative errors for pressure and velocity as follows:

$$\text{Err}\, p = \frac{\sum_{N,M} |p - p^*|}{\sum_{N,M} |p^*|}, \quad \text{Err}\, u = \frac{\sum_{N,M} |u_x - u_x^*| + |u_y - u_y^*|}{\sum_{N,M} |u_x^*| + |u_y^*|} \tag{35}$$

DOI: 10.1002/fld

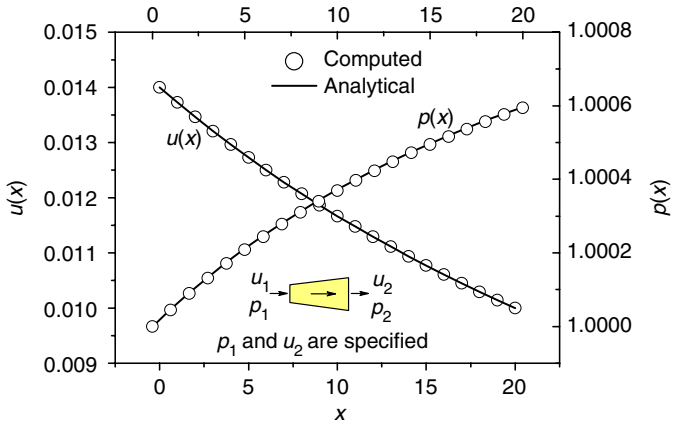

Figure 4. Velocity and pressure distributions in Case F.

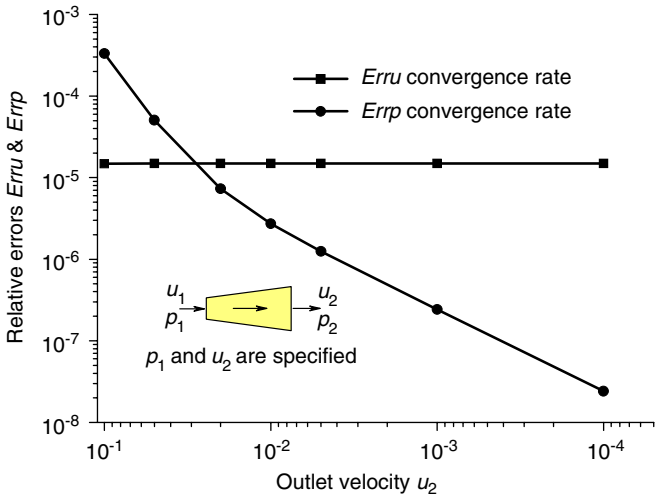

Figure 5. Error dependence on compressibility.

where p, u_x and u_y are the lattice pressure, velocity component in the x-direction and velocity component in the y-direction on the $N \times M$ lattice, respectively, and those with asterisk superscripts are the analytical solutions.

Based on the same parameters as in Case C or Case F, the compressibility effect is analysed by only reducing the outlet velocity u_2. Figure 5 shows the dependence of errors Err u and Err p on u_2. It is clear that Err u does not change, but Err p decreases rapidly as u_2 decreases. This is because the momentum equation (25) has a compressibility error term $O(M^3)$, but the continuity equation (24) does not.

DOI: 10.1002/fld

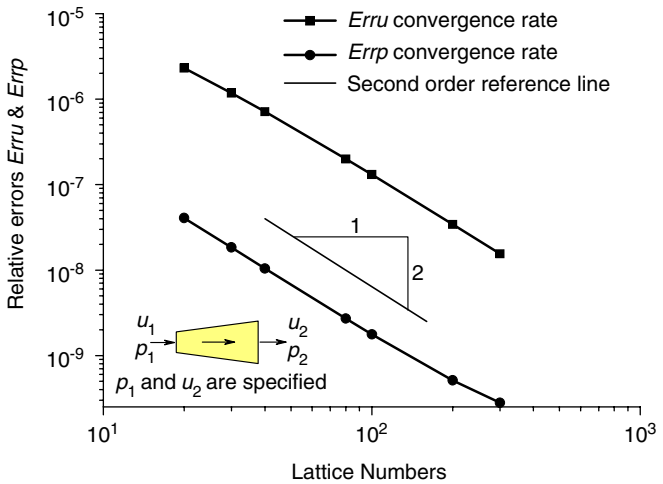

Figure 6. Lattice resolution dependence analysis.

3.2.2. Convergence order analysis. To analyse the lattice convergence, different lattice numbers are chosen to simulate a case with the same parameters as in Case A, except for $u_2 = 0.001$. The smaller u_2 is selected specially to eliminate the compressibility effect. Figure 6 shows the trendlines of error change along lattice resolution, in which second-order convergence rates are evident for both Err u and Err p, corresponding well to the error term $O(\delta_t^2)$ in Equations (24) and (25). Because the compressibility error is reduced, the relative error of pressure becomes smaller than that of velocity. The two errors are extremely small, for instance, when $N = 100$, Err u and Err p equal 1.3×10^{-7} and 1.8×10^{-9}, respectively.

From the above analysis, one may conclude that the proposed scheme is accurate for non-uniform but steady source term problems.

3.3. Unsteady flow

To verify the simulation ability concerning unsteady and non-uniform source terms, a water hammer case with similar layout to Case F, namely $\rho_0 = 1$, $h_1 = 1$, $h_2 = 1.4$ and $a = 0.02$, is suitably chosen. This example is also typical because its source terms are not only unsteady, but also non-uniform. Initially the fluid in the duct is still, and after the simulation starts, the pressure at the inlet holds constant at $p_1(t) = 1.0$, while the velocity at the outlet increases linearly to 0.1 within the first 100 LBM time steps, and remains constant thereafter. In this way, a typical transient flow governed by Equations (29) and (30) is generated. The characteristics of pressure wave transmission and reflection are similar to those in the penstocks of hydropower plant after unit starting.

Model D2Q9 is used on a $N \times M = 20 \times 10$ lattice. Because no analytical solutions are available, we adopt the method of characteristics (MOC) in Reference [24] to obtain accurate one-dimensional numerical results for comparison. To ensure stability of simulations, MOC leaves out the convection and viscosity terms in the momentum equation (30), and accordingly D2Q9 cancels the convection term in (25) and uses a very small viscosity $v = 0.0001$.

DOI: 10.1002/fld

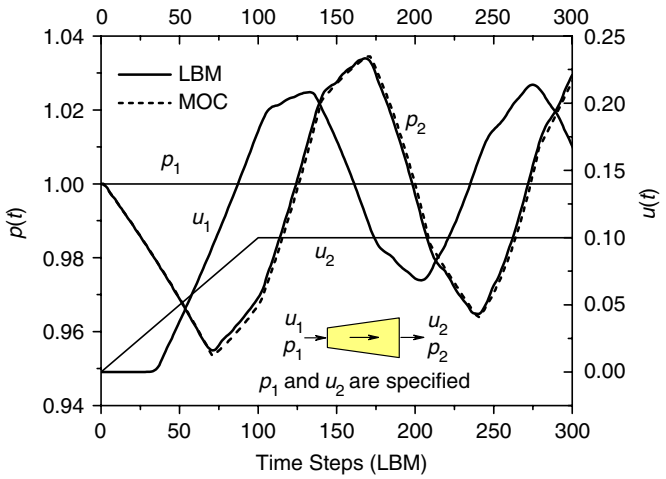

Figure 7. Comparison of outlet pressure histories of LBM and MOC.

The histories of pressures and velocities at the duct inlet and outlet are demonstrated in Figure 7, from which the very good agreement between the outlet pressure lines of the two methods can be seen.

The MOC solutions are of high accuracy [24], therefore, the good agreement suggests that the proposed scheme is also accurate for unsteady and non-uniform source term problems.

4. CONCLUSIONS

This paper proposes a scheme to introduce unsteady and non-uniform source terms into the lattice Boltzmann model. The idea is described by a theoretical derivation and the accuracy is verified by typical examples. It is shown that the approach is general, not only for, respectively, treating the force term in the momentum equation and the source term in the continuity equation, but also for a synchronous consideration of both. Moreover, the source terms can be unsteady or steady, and non-uniform or uniform. The second-order convergence feature, which is demonstrated by both analytical and numerical verifications, accords well with the intrinsical accuracy of LBM. Though these are achieved by way of adding extra terms to the LBE, it can be easily implemented, however, by other ways, such as revising the equilibrium functions.

ACKNOWLEDGEMENTS

This work is supported by the National Natural Science Foundation of China (NSFC, Grant numbers 50009007 and 10572106) and by the Scientific Research Foundation for Returned Overseas Chinese Scholars, State Education Ministry, China.

REFERENCES

1. Chen S, Doolen GD. Lattice Boltzmann method for fluid flows. *Annual Review of Fluid Mechanics* 1998; **30**:329–364.

DOI: 10.1002/fld

2. Mason RJ. A multi-speed compressible lattice-Boltzmann model. *Journal of Statistical Physics* 2002; **107**:385–400.
3. Lallemand P, Luo L-S. Theory of the lattice Boltzmann method—acoustic and thermal properties in two and three dimensions. *Physical Review E* 2003; **68**(036706):1–25.
4. Sullivan SP, Gladden LF, Johns ML. 3D chemical reactor LB simulations. *Mathematics and Computers in Simulation* 2006; **72**:206–211.
5. Zheng HW, Shu C, Chew YT. A lattice Boltzmann model for multiphase flows with large density ratio. *Journal of Computational Physics* 2006; **218**:353–371.
6. Onishi J, Chen Y, Ohashi H. Dynamic simulation of multi-component viscoelastic fluids using the lattice Boltzmann method. *Physica A* 2006; **362**:84–92.
7. Xuan YM, Yao ZP. Lattice Boltzmann model for nanofluids. *Heat Mass Transfer* 2005; **41**:199–205.
8. Breyiannis G, Valougeorgis D. Lattice kinetic simulations of 3-D MHD turbulence. *Computers and Fluids* 2006; **35**:920–924.
9. Cheng YG, Zhang SH, Chen JZ. Water-hammer simulations by the lattice Boltzmann method. *Journal of Hydraulic Engineering* (*SHUI LI XUE BAO*) 1998; **29**(6):25–31 (in Chinese).
10. Cheng YG, Suo LS. 2D open channel flow simulations by the lattice Boltzmann model. *Advances in Water Sciences* 2003; **14**(1):9–14 (in Chinese).
11. Zou Q, Hou S, Doolen GD. Analytical solutions of the lattice Boltzmann BGK model. *Journal of Statistical Physics* 1995; **81**:319–334.
12. Luo L-S. Theory of the lattice Boltzmann method: lattice Boltzmann models for nonideal gases. *Physical Review E* 2000; **62**(4):4982–6996.
13. Buick JM, Greated CA. Gravity in a lattice Boltzmann model. *Physical Review E* 2000; **61**(5):5307–5320.
14. Li B, Kwok DY. A lattice Boltzmann model with high Reynolds number in the presence of external forces to describe microfluidics. *Heat and Mass Transfer* 2004; **40**:843–851.
15. Guo Z, Zheng C, Shi B. Discrete lattice effects on the forcing term in the lattice Boltzmann method. *Physical Review E* 2002; **65**(046308):1–6.
16. Chen S, Liu Z, Shi B, Zhang C. External body force in finite difference lattice Boltzmann method. *Journal of Hydrodynamics*, *Series B* 2005; **17**(4):473–477.
17. Lu Y, Zhan J. Comparison between different boundary treatments and between different body force term expressions in lattice Boltzmann method. *Acta Scientiarum Naturalium Universitatis Sunyatseni* 2006; **45**(3): 22–26 (in Chinese).
18. Cheng YG, Suo LS. A lattice BGK model for simulating one-dimensional unsteady open channel flows. *Advances in Water Sciences* 2000; **11**(4):362–367 (in Chinese).
19. Peskin CS. The immersed boundary method. *Acta Numerica* 2002; **11**:479–517.
20. Feng ZG, Michaelides EE. The immersed boundary-lattice Boltzmann method for solving fluid-particles interaction problems. *Journal of Computational Physics* 2004; **195**:602–628.
21. Halliday I, Hammond LA, Care CM, Good K, Stevens A. Lattice Boltzmann equation hydrodynamics. *Physical Review E* 2001; **64**(011208):1–8.
22. Frisch U, d'Humières D, Hasslacher B, Lallemand P, Pomeau Y, Rivet J-P. Lattice gas hydrodynamics in two and three dimensions. *Complex System* 1987; **1**:649–707.
23. Cheng YG, Suo LS. Lattice Boltzmann scheme to simulate 2-D hydraulic transients in concrete spiral cases. *XXIX IAHR Congress*, vol. 9. Beijing, China, 2001; 710–718.
24. Wylie EB, Streeter VL, Suo LS. *Fluid Transients in Systems*. Prentice-Hall: Englewood Cliffs, NJ, 1993; 37–44.

DOI: 10.1002/fld